Available online at www.sciencedirect.com
SCIENCE DIRECT
Wear 260 (2006) 287–295
WEAR
www.elsevier.com/locate/wear

Carbon based tool coatings as an approach for environmentally friendly metal forming processes

F. Klocke [a], T. Maßmann [a,*], K. Bobzin [b], E. Lugscheider [b], N. Bagcivan [b]

[a] *Chair of Manufacturing Technology, Laboratory for Machine Tools and Production Engineering (WZL), RWTH Aachen University, Steinbachstraße 53, 52074 Aachen, Germany*
[b] *Materials Science Institute, RWTH Aachen University, Augustinerbach 4-22, 52062 Aachen, Germany*

Received 18 November 2004; received in revised form 13 April 2005; accepted 22 April 2005
Available online 1 August 2005

Abstract

The deep-drawing of austenitic stainless steel AISI 304 provides a considerable challenge for production engineers. A major problem in such processes is adhesive tool wear which is often prevented using chlorous mineral oils. The aim of this work was to replace these hazardous lubricants with biodegradable, rape oil based fluids. For that purpose a modified triglyceride named HIGTO(I) is used in combination with a graded zirconium carbide (ZrC_g) physical vapour deposition (PVD) tool coating chosen because of their good performance in previous studies. The results from deep-drawing tests with uncoated dies show that HIGTO(I) itself is not able to replace chlorous deep-drawing oils. But in combination with HIGTO(I) as a lubricant and ZrC_g as tool coating deep-drawing forces are reduced and adhesive tool wear is prevented. This combination even exceeds the performance of chlorous deep-drawing oils. The wear effects, which appeared in different tests, could be explained by an analysis of tool loads and process temperatures, calculated using FE-simulations.

Keywords: Deep-drawing; Austenitic stainless steel; Graded zirconium carbide; Carbon based tool coatings

1. Introduction

The collaborative research center 442 “Environmentally Friendly Tribosystems” (SFB 442) has the aim to apply biodegradable lubricants in all parts of a machine tool. This project which has been funded by the German Science Foundation (DFG) is concerned with all machine parts like hydraulic components, bearings or guides and the lubrication of cutting and forming tool and dies. For this purpose rape oil based ester has been chemically modified to combine the good lubricating properties of a native ester with high oxidation and hydrolysis stability [1,2].

One of the forming processes which has been chosen for the evaluation of this new lubrication system is the cup deep-drawing of austenitic stainless steel AISI 304. In many cases chlorous mineral oil based lubricants are used to reduce the adhesive wear which typically appears on forming dies when processing this material [3].

In this work, a modified triglyceride named HIGTO(I) was used to replace chlorous mineral oil because of its good performance in previous studies [1,2]. This substance is a modification of GTO (glycerin tri oleate) with Isobutanol leading to hydroxy isobutoxi glycerin tri oleate (HIGTO). The modification is an addition reaction of isobutanol to the unsaturated double bonds of oleochemical’s fatty acid chains, using the corresponding epoxid as an intermediate.

Deficiencies in tribological performance must be compensated by physical vapour deposition (PVD) tool coatings. From literature it is known that carbon based coatings offer high potential for sheet metal forming operations [4]. A graded zirconium carbide (ZrC_g) tribological physical vapour deposition coating has been developed at Materials Science Institute in Aachen within the collaborative research center SFB442. The aim of this coating is to reduce friction and to protect against wear. The use of such coatings on components

* Corresponding author. Tel.: +49 241 80 27428; fax: +49 241 80 22293.
E-mail address: T.Massmann@wzl.rwth-aachen.de (T. Maßmann).

0043-1648/$ – see front matter © 2005 Elsevier B.V. All rights reserved.
doi:10.1016/j.wear.2005.04.026

like roller bearings and gear wheels is proven [5]. The use on deep-drawing dies is still at an early stage. The combination of good adhesive properties and high strength at high elastic deformation, as well as very low coefficients of friction, have made carbon layers the structural elements of several modern tribological systems [6]. Due to the graded carbon content ZrC_g has a predefined hardness distribution, which reaches its maximum in the center of the coating. The latter area has a superstoichiometric carbon content with a topmost layer of pure carbon which acts as a solid lubricant for closed tribological systems like bearings. Due to these factors the first investigations have focused on ZrC_g. As a result of this investigation, requirements have been identified for future coating development.

2. Experimental and simulative methods

2.1. Deposition process

2.1.1. Description of coating equipment

The drawing dies were coated in a semi industrial plant, PVT 550, using a magnetron sputter ion plating (MSIP) process in dc mode. The power supply can also be applied to the substrate to offer plasma etching of substrate and coating with a bias voltage. The flow of process gas and reactive gas is regulated by a process computer. In addition, control of gradation during the coating and monitoring of the overall coating process is done by the process computer as well. In order to position the substrate at the required distance of 60 mm from the target surface a movable table is used. A side shield is attached for protection of the substrate from impurities during sputter cleaning of target.

2.1.2. Substrate preparation

A decisive aspect for successful low-temperature coating is the preparation and especially the cleaning of the substrate before deposition. Therefore, the polished specimens were first cleaned with isopropanol to remove any adherent grease. Following, the samples were cleaned in a semi industrial washing line at 55 °C with several stages using ultrasonic baths with Galvex SU 93, a surface active wetting agent in aqueous solution, from NGL cleaning technology. Finally, the samples were immersed in deionised water before they were rinsed with isopropanol and dried with nitrogen. In situ cleaning was done by Argon R.F.-Plasma etching at 1 Pa with a high-frequency voltage of 750 V for 30 min.

2.1.3. Deposition parameters

Table 1 lists the most important deposition parameters. Gradation of coating is obtained by a linear increase of reactive gas flow until a soft-shearing layer of 100% carbon develops as the topmost layer. The stoichiometric hard material phase forms during deposition at a carbon content of 38–50 % [7]. Deposition of pure Zr in the beginning ensures a good bonding between substrate and coating by a pure metallic bondcoat. Fig. 1 shows the gradation of reactive gas flow. The substrate material, hardened cold working-steel AISI D2 with a hardness 62 HRC, required a configuration of deposition parameters with regard to its temperature-sensitivity.

Table 1
Deposition parameters for graded ZrC_g coatings

Substrate material	X155CrVMo12-1 (AISI M3:2)
Target material	Zirconium 99%
Process gas	Argon
Reactive gas	Acetylene (C_2H_2)
Reactive gas share	0–14%
Gas pressure	1 Pa
Target power density	78.5 W/cm^2
Bias voltage	Self bias
Coating time	24 min

2.2. Coatings characterisation

2.2.1. Physical/mechanical properties

Adhesion behaviour was examined with calo-testing and Rockwell hardness testing. Calo-testing was done using a steel ball with a radius of 10 mm and diamond suspension with a grain size of 1 μm as abrasive medium. Rockwell hardness testing was performed with load C (1471 N) and the adhesion was characterised according to VDI (Verein Deutscher Ingenieure) guideline no. 3198. A quantitative analysis of adhesion behaviour was achieved by scratch testing. Several scratches created with different loads were examined to determine the critical load.

2.2.2. Advanced properties

Additional characterisation of the ZrC_g coating was done by an analysis of wetting behaviour. The spreading coefficient describes the difference between the adhesion energy between two phases and the cohesive energy between the molecules within a phase. Calculation of spreading coefficient requires that surface energies of solids as well as surface energies of fluids have to be experimentally determined. A detailed presentation of theory can be found in [8]. The required tests of surface energy of fluids (pendant drop) and solids (sessile drop) were done with a Krüss DSA 10 video contact angle measuring device.

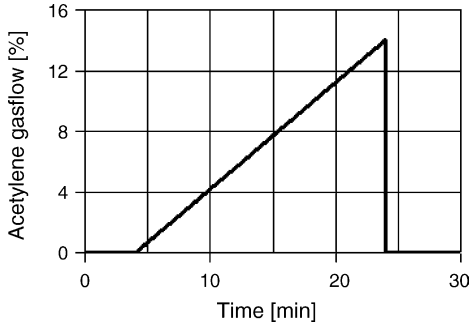

Fig. 1. Reactive gas flow.

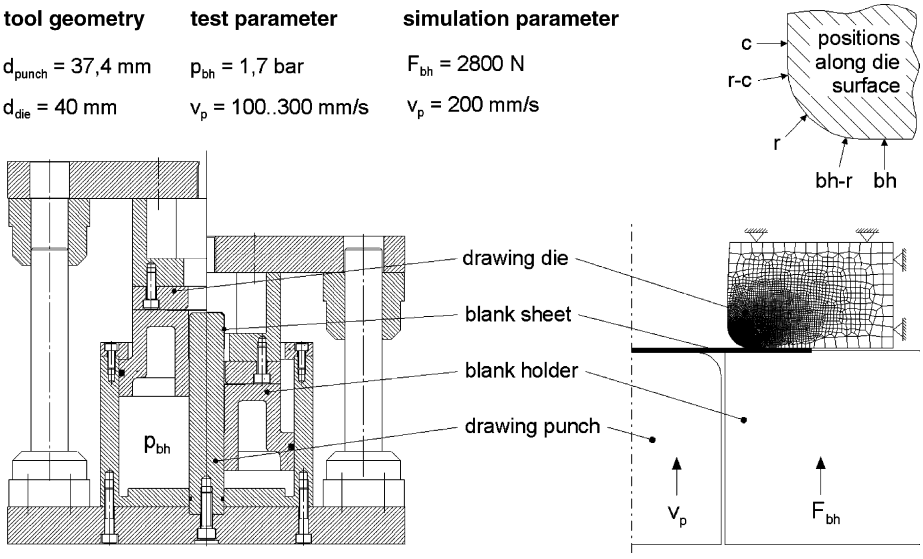

Fig. 2. Setup of cup deep-drawing tool and the appropriate FE-model, upper right: abbreviations for different positions along the die surface.

For a proper realisation of the tests, samples were first cleaned in acetone and then in isopropanol in an ultrasonic bath for five minutes. Finally, they were dried with nitrogen. Five liquids covering the widest possible range from very polar (water) through to almost completely disperse (diode methane) were used to determine the surface energy of solids. In order to guarantee statistically correct results a minimum of 900 contact angles were acquired. Therefore, 60 contact angles per drop and 3 drops per liquid were investigated. Finally, spreading coefficient of each combination of fluid and solid was calculated according to [8]. In a first step surface energies of solids were determined. The investigated specimens were of the coated cold working steel (AISI D2 with ZrC_g) and high speed steel (AISI M3:2). Samples were coated with ZrC_g and polished, respectively.

2.3. Deep-drawing tests and simulation

One of the forming processes which have been chosen for the evaluation of the new lubricants and tool coatings is the cup deep-drawing of austenitic stainless steel AISI 304. The results of these tests are the wear appearance, which had to be analysed using SEM microscopy, and the measured forces, which give an idea of the different behaviour in friction. In addition, 2D-FE-simulations of the cup-deep-drawing process have been made using the software DEFORM in order to correlate the test results with the dominating mechanical and thermal die loads. This proceeding was found to be useful within the analysis of tribological mechanisms [9].

The tests were carried out on a mechanical 630-t press (type: Schuler KB-630). The set-up of the deep-drawing tool and the accompanying FE-simulation are shown in Fig. 2. The sheet blanks had a thickness of 1 mm. The diameter of punch and die were chosen as $d_{\text{punch}} = 37.4$ mm and $d_{\text{die}} = 40$ mm, respectively. The dies have a drawing radius of 5 mm.

The blank holder operates with a pneumatic pressure p_{bh} of 1.7 bar. With a compression-loaded area of 16475 mm^2 this results in a blank holder force F_{bh} of 2800 N which was used as the blank holder movement control in the simulation.

Because of the mechanical press drive the process speed falls from 300 mm/s at the beginning to 100 mm/s at the end of the drawing process. For the simulation an average speed of 200 mm/s has been chosen.

Within the FE-model the stainless steel blank sheet has a plastic material behaviour with strain hardening. The used flow curves were determined for the temperatures 25, 85 and 150 °C using tensile tests according to the standard DIN EN 10002 [10]. The drawing die is designed as an elastic object. The other tools, the punch and the blank holder, are not analysed in this work and are defined as rigid objects.

Along the die radius five positions have been defined for a better orientation (see Fig. 2). The position bh describes the plane surface area which is parallel to the blank holder surface, r means the radius and c the cylindrical part of the die. Between these positions bh–r and r–c stand for the transition areas.

3. Results

3.1. Coating properties

3.1.1. Chemical composition

The development of carbon content in the coating and the chemical composition of ZrC_g coating are described in detail in [11]. Glow discharge optical emission spectroscopy (GDOES) shows that the carbon content increases during deposition. Carbon content reaches its maximum at the end of the deposition process, when a pure carbon layer is deposited. At the same time content of zirconium decreases

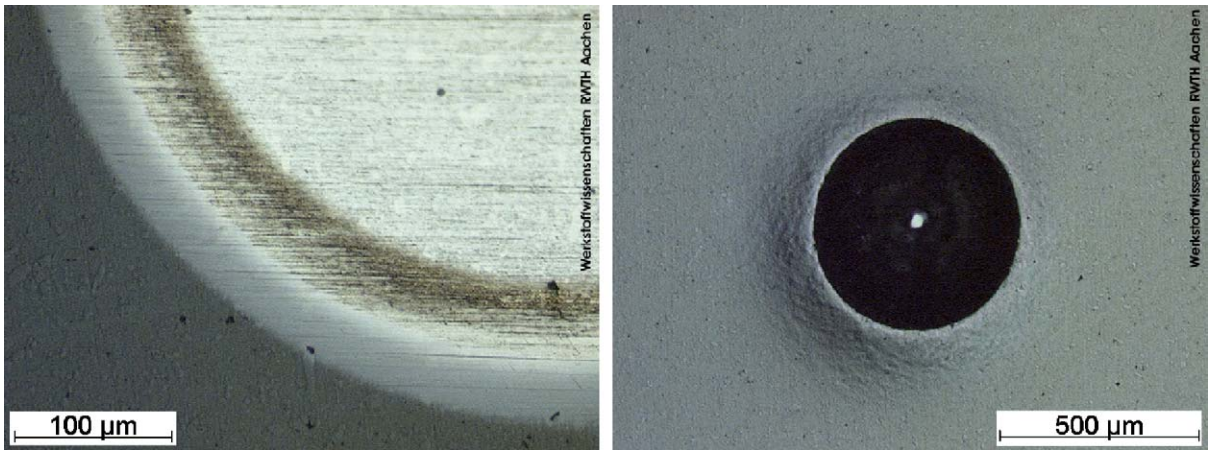

Fig. 3. Characterization of adhesion behaviour in the ball on plate abrasive Calo-test and the Rockwell-test.

with increasing coating thickness. Zirconium content has its maximum at the beginning of deposition process when a purely zirconium bond coat is deposited. From the phase diagram of zirconium and carbon it is known that there is a stoichiometric phase in between 38 and 50 at.% carbon content.

3.1.2. Physical/mechanical properties

The calo-test and the Rockwell hardness test revealed excellent adhesion of substrate and coating. Fig. 3 shows the good behaviour of the ZrC_g coating in terms of adhesion and stress resistance. The different phases of zirconium and carbon which form due to the increase in reactive-gas flow during the deposition process are observed as concentric circles in the micrograph of the calo-test. The overall thickness of coating is determined as 2 μm with a 0.9 μm thick bondcoat. In the Rockwell test (HRC) adhesion class 1 (very good) was achieved. The micrograph of the HRC impression displays neither cracks nor adhesive failures. During the scratch-test failure in the composite was observed the first time at a load of 35 N.

3.1.3. Advanced properties

Figs. 4 and 5 show the resulting surface energies of tested materials and fluids. ZrC_g coating reveals a higher disperse share than polar share. In contrast to the coating uncoated AISI M3:2 steel is predominantly polar. Both fluids show a high disperse share.

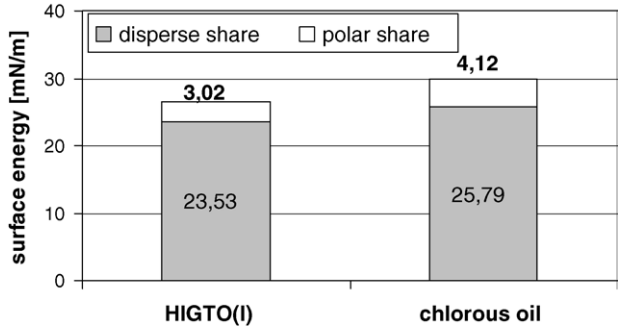

Fig. 5. Surface energy of tested fluids.

Fig. 6 shows the spreading coefficients for varying pairings. Wetting of fluids on solids only occurs for positive spreading coefficients and is proportional to spreading coefficient. Thus, with increasing spreading coefficient more fluid will spread over the surface and wetting will increase [12]. The results show that the highest spreading coefficient was reached with HIGTO(I) on ZrC_g coating. Therefore, this combination will result in an improved wetting condition

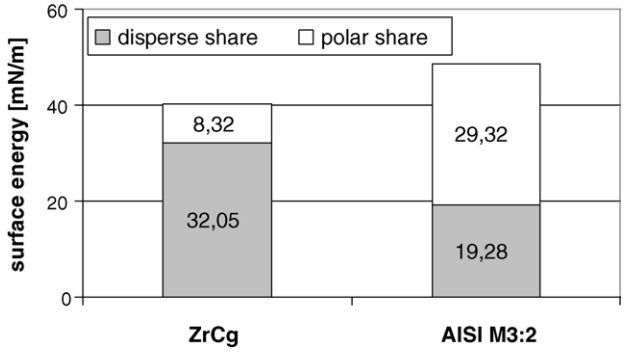

Fig. 4. Surface energy of tested solids.

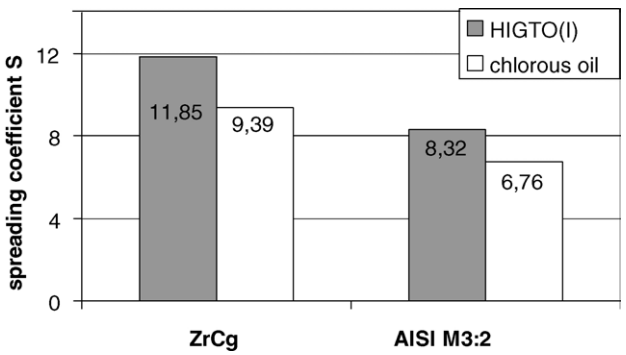

Fig. 6. Calculated spreading coefficients *S* for tested solids and fluids.

Table 2
Deep-drawing tests

Die no.	Die material	Coating	Lubricant	d_{blank} (mm)	Strokes
1	AISI M3:2	–	Chlorous mineral oil	75	70
2	AISI M3:2	–	HIGTO(I)	75	8
3	AISI D2	ZrC_g	HIGTO(I)	75	5
4	AISI D2	ZrC_g	HIGTO(I)	60	70

relative to the currently used combination of tool material and lubricant (AISIM3:2 and chloric oil).

3.2. Deep-drawing tests

The purpose of the tool coatings applied in this work is to make the use of biodegradable lubricants in deep-drawing operations possible. Before the application and testing of these new tool coatings can be conducted, it is important to know how the tribological behaviour of the newly developed lubricant differs from conventional lubricants. For that reason, two identical uncoated dies of AISI M3:2 have been tested with two of above described fluids (chlorous mineral oil and the synthetically modified ester named HIGTO(I)). In these first tests a blank diameter d_{blank} of 75 mm was used. After that two dies of AISI D2 were coated with ZrC_g and tested in combination with HIGTO(I), but with different blank diameters. Table 2 gives an overview of all tests.

3.2.1. Wear behaviour

The SEM-micrographs of the two uncoated drawing dies 1 and 2 in Fig. 7 show the previously defined areas close to the drawing radius. With the first die 70 cups have been produced using the chlorous mineral oil. After that it can be observed that workpiece material adheres at the tool surface in the positions bh–r and r–c. Aside from these two positions no wear could be detected.

The second die which was lubricated with HIGTO(I) shows massive adhesion in the cylindrical part (Fig. 7 lower right, position c) even after the first eight cups. Because of this the test was aborted in this early stage. Whereas the wear in the area bh–r looks quite similar to that on the first die, the adhesion on the inner part of this die is not limited to the position r–c but spreads down to the cylindrical part. It is obvious that the biodegradable lubricant HIGTO(I) offers a lower wear protection than the chlorous mineral oil.

In the following it should be proven whether the ZrC_g-coating, which was initially developed for components of a machine tool, could take over the wear preventive properties of the lubricant.

In a first try-out a die of hardened cold working-steel AISI D2 was coated with ZrC_g and tested using HIGTO(I) for lubrication (die 3). The blank diameter d_{blank} again was set to 75 mm. After the first stroke serious delamination of the coating was recognised in the area bh–r as can be seen in the upper part of Fig. 8. After a total of five strokes the test was aborted. In contrast to the tests with uncoated tools no adhesion took place in the cylindrical part, although the surface look changes in that region.

After that another coated die was tested under the same lubrication conditions. But now the blank diameter of 75 mm was reduced to 60 mm in order to see the coating behaviour under lower mechanical loads. As can be seen in the bottom

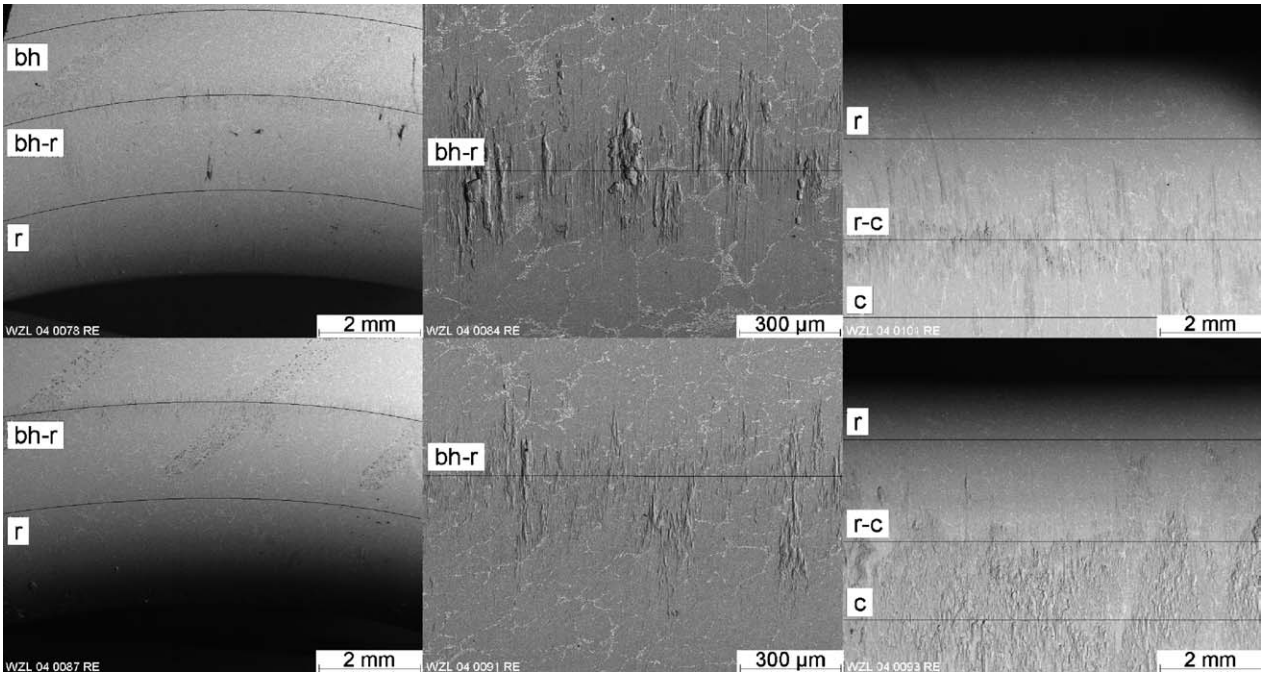

Fig. 7. SEM-pictures of worn reference tools (uncoated AISI M3:2), upper: lubricated with chlorous mineral oil (70 strokes), lower: lubricated with HIGTO(I) (8 strokes).

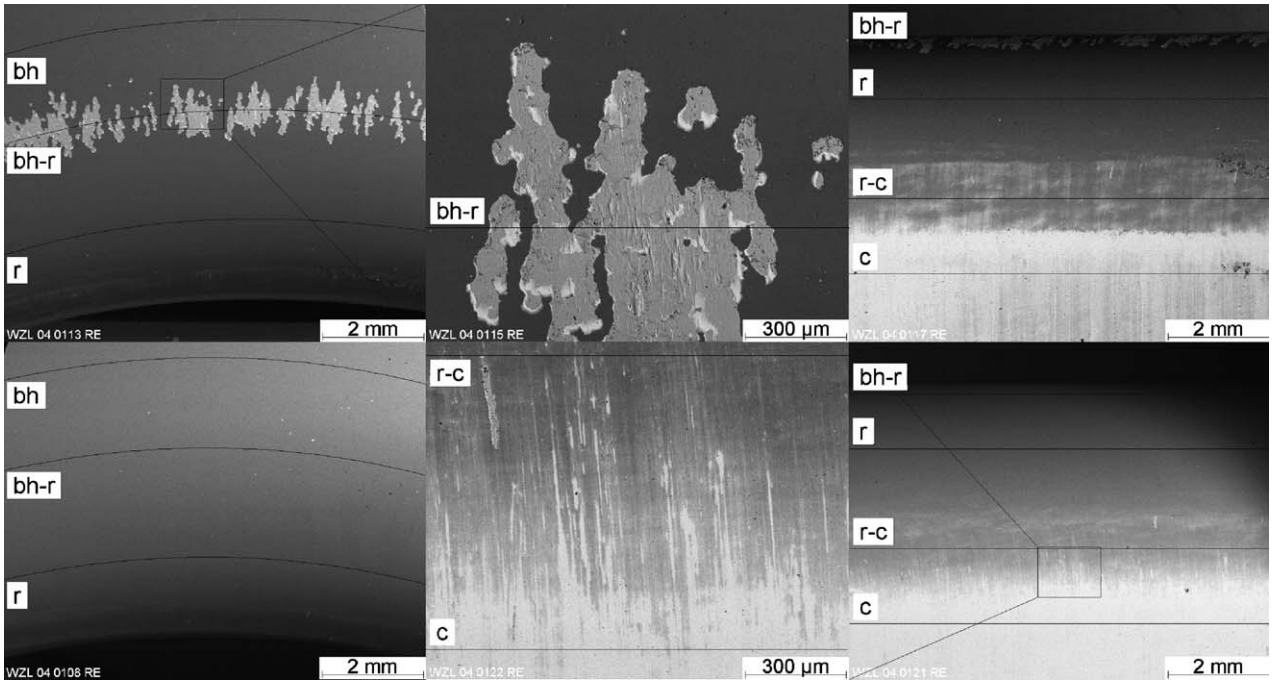

Fig. 8. SEM-pictures of worn die coatings (ZrCg on AISI D2 lubricated with HIGTO(I)), upper: blank diameter d_{blank} = 75 mm (5 strokes), lower: d_{blank} = 60 mm (70 strokes).

part of Fig. 8 no coating delamination takes place even after a total of 70 strokes.

However, in the cylindrical part of both coated dies (Fig. 8, upper and lower right) the coating did not fail. After the first stroke, the coating looks brighter. But during the following strokes the appearance of the coatings does not change anymore. The SEM-analysis proved that the coating is still existent. This could be verified with an energy dispersive X-ray (EDX)-analysis which detected a distinctive amount of zirconium in the area c of both dies. It seems that the soft top layer of the ZrC_g-coating was abraded (see Fig. 8 lower middle). But the remaining coating is still enough to prevent the formation of adhesive wear as no workpiece material could be detected in this area.

3.2.2. Drawing forces

Aside from the wear scars the drawing forces were measured in all conducted tests. The left diagram in Fig. 9 shows the maximum drawing forces for the first five strokes of the uncoated dies and the first coated die. So this diagram represents the tests which were conducted with the large blanks (d_{blank} = 75 mm). It can be seen that the lowest forces were for a coated die in combination with HIGTO(I). The chlorinated oil also leads to low forces but it needs one press stroke for activation. HIGTO(I) itself leads to quite high drawing forces.

The right diagram in Fig. 9 shows the results from the two longer test series in which no massive wear effects took place. Although the force values are very different the course of maximum force over time can be evaluated. Whereas the chlorous oil shows a constant behaviour, the combination of ZrC_g and HIGTO(I) reduces the forces after some strokes. This trend goes on until the last stroke (70 overall). Overall a reduction of 20% could be achieved from the first to the last stroke.

3.3. Simulation results

FE-simulations of the drawing process have been conducted in order to find additional explanations for the

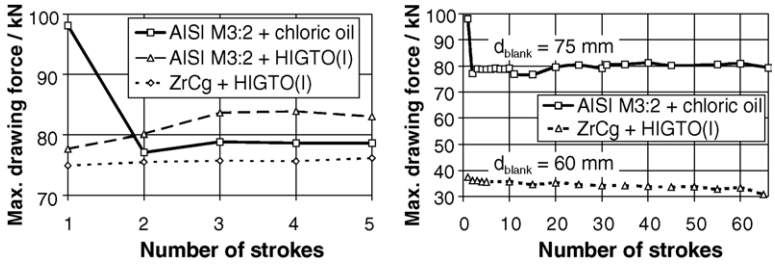

Fig. 9. Maximum drawing forces.

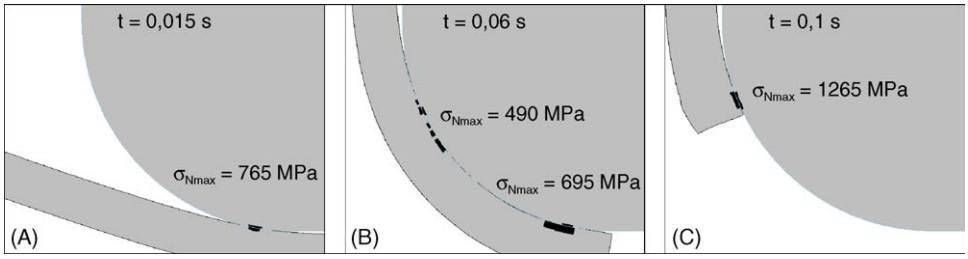

Fig. 10. Contact situation between die and workpiece (d_{blank} = 60 mm) at different time steps: contact area (black) and maximum contact normal stress σ_{Nmax} inside the contact area.

observed wear effects. First of all the FE-results explain why the wear is limited to certain positions.

Fig. 10 shows the contact situation between die and workpiece for three representative drawing stages. At the beginning of the process, the blank holder force F_{bh} is applied onto the sheet and the punch starts moving upwards. At this point of time the contact area is limited to one point in the position bh–r (Fig. 10A).

This contact area exists until the workpiece edge passes. It causes contact normal stresses σ_N on the die surface up to more than 700 MPa. In this area, adhesive wear takes place even when using the chlorous lubricant (Fig. 8, middle). In the middle of the process, a second contact takes shape between the positions r and r–c (Fig. 10B). The contact stresses are lower than in the position bh–r which results from the larger dimension of the contact area. When the sheet edge passes r, this contact area shrinks to another point-contact in the surrounding of position r–c and the surface loads rise significantly (Fig. 10C).

As Figs. 7 and 8 show wear effects take place in the positions bh–r, r–c and c. For these positions some more results are displayed here. In Table 3, the calculated maximum effective stresses according to von Mises are given. In comparison with Fig. 10, it can be seen that the maximum effective stress appears in the position bh–r whereas the contact stress is quite low in this area.

Fig. 11 displays the calculated temperatures for the points as functions of process time. It is obvious that the highest temperatures are calculated for position c.

4. Discussion

The different test results are discussed in the following. In doing so the FE-results are taken into account.

Table 3
Calculated effective die stress σ_{Vmax} for different positions

d_{blank} (mm)	Position	σ_{Vmax} (MPa)
60	bh–r	525
	r–c	365
	c	373
75	bh–r	632
	r–c	500
	c	305

4.1. Lubricant behaviour

The first deep-drawing tests (dies 1 and 2) showed that the newly developed rape seed oil based lubricant HIGTO(I) cannot exceed the performance of a conventional chlorous deep-drawing oil when conventional uncoated dies are used. It causes strong adhesive wear and high drawing forces.

4.1.1. Wear behaviour

The difference between the wear in the cylindrical part of dies 1 and 2 can be explained with the temperatures which emerge from dissipated forming energy and from friction and their influence on the lubricant. Looking at the FE-results, it becomes clear that only in the cylindrical part of the die temperatures are high enough to activate the chlorine additives. The chlorine reacts with the iron of the tool to iron chloride ($FeCl_2$ and $FeCl_3$) which leads to the actual good tribological conditions. This chemical reaction, however, starts only at temperatures above 100 °C [3]. This explains, why there are wear effects in the contact areas bh–r and r–c but not in the contact area c. This indicates that the base fluids themselves (both, chlorous mineral oil and HIGTO(I)) cannot prevent wear development, but only the chlorous additives.

4.1.2. Drawing forces

In Fig. 9, the maximum drawing forces for the first five strokes of both tests are compared. The first stroke using the chlorous mineral oil leads to the highest measured force of all tests. The reason for this phenomenon is the chlorous additive. Because of the low temperature in the beginning

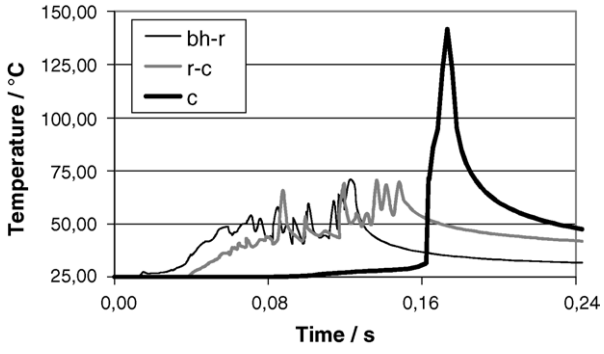

Fig. 11. Calculated surface temperature.

(about 20 °C) the die is not protected by iron chloride during the first stroke [3]. Once an iron chloride film has formed on the die surface, the drawing forces are reduced. It can be seen that HIGTO(I) leads to higher forces which is obviously caused by the serious adhesive wear formation.

4.2. Coatings behaviour

Two tests have been conducted with ZrC_g coated dies using HIGTO(I) for lubrication and blanks of different diameters. Although the coatings seem not to be applicable for high tool loads which appear when using the larger blanks, it reduces adhesive wear and lowers tool forces.

4.2.1. Wear behaviour

As could be found in the SEM analysis of dies 3 and 4 (Fig. 8) the ZrC_g coating is able to prevent adhesive wear at the dies, but the coatings themselves are worn. It has to be distinguished between coating delamination and coating abrasion or burnishing.

The coating delamination on die 3 results from the contact situation which dominates at the beginning of the process between sheet and die. The contact is limited to a close line in the position bh–r. The above described FE-simulation showed that the value of effective stress in this point is about 20% higher for the large blank (die 3) than for smaller one (die 4). This could be a reason for coating failure on die 3. However, it is strange that the contact stresses are quite low in this position. In future, it should be analysed in more detail which stress states are responsible for the coating delamination.

In the position c, the contact stress is much higher than in position bh–r while the effective stress is lower. Nevertheless, the coating did not fail on both dies (dies 3 and 4). Instead of that the surface is burnished which gives it a brighter look in SEM analysis, as it can be seen in Fig. 8. This running-in effect needs only one press stroke. After that the surface seems not to alter any more. EDX analysis of dies 3 and 4 showed neither adhesion of workpiece material nor substrate material which would indicate a coating failure.

4.2.2. Drawing forces

Although the coating delaminates after the first stroke in the area bh–r of die 3 the friction reduction is enough to lower forces and to exceed even the tests with chlorous mineral oil (Fig. 9, left diagram). However, the measured forces for the different combinations of die material and lubricant correlate with the determined spreading coefficients in Fig. 6. The wetting behaviour of materials and fluids seems to have an influence on the friction forces inside the drawing process.

The test with the coated die and the small blanks (d_{blank} = 60 mm, die 4) of course leads to much lower forces (Fig. 9, right diagram). But compared with the mineral oil lubricated test, however, another effect can be observed. With chlorous mineral oil (die 1) the maximum drawing force stays quite constant for all strokes. Changes could also be recognised between first and second stroke. But the maximum force is reduced continuously when using the coated die number 4 in combination with HIGTO(I). This may be related to the abrasion of the coatings toplayer. This intended running-in effect is due to the gradation of ZrC_g coating.

5. Conclusions

The combination of a newly developed lubricant HIGTO(I) with a graded tool coating ZrC_g showed good results in this pilot survey. The low polar share of the coating's surface energy, the good spreading behaviour of HIGTO(I) on the coating and the running-in behaviour of the coatings lead to low process forces and a distinctive reduction of adhesive wear. Besides these positive results it has to be noted that the coating delaminated under higher tool loads which result from a higher draw depth. Further activities in coating development should aim at higher adhesion between tool and coating. In addition, the stress state which caused this delamination should be analysed more detailed to identify other approaches.

Acknowledgement

The authors gratefully acknowledge the financial support of the Deutsche Forschungsgemeinschaft (DFG), SFB 442 within the project "Environmentally Friendly Tribosystems", see also www.dfg.de.

References

[1] F. Klocke, T. Maßmann, D. Breuer, Environmentally friendly lubricants for cold forming processes, in: International Cold Forging Conference, Columbus, Ohio, USA, September 2003.
[2] F. Klocke, T. Maßmann, P. Weckes, L.A. Rios, H. Schuster, W.F. Hölderich, On the tribological performance of newly developed rape oil based biodegradable lubricants for cold forging processes, production engineering, Ann. German Acad. Soc. Prod. Eng. XI 2 (2004) 75–78.
[3] T. Mang, W. Dresel, Lubricants and Lubrication, Wiley-VCH, Weinheim, 2001.
[4] K. Taube, Carbon-based coatings for dry sheet-metal working, Surf. Coat. Technol. 98 (1998) 976–984.
[5] P.W. Gold, J. Loos, M. Kuhn, Wear and friction characteristics of PVD-coated roller bearings, Surf. Coat. Technol. 177-178 (2004) 469–476.
[6] J. Brand, Tribologische Schichten, metalloberfläche (mo) 52 (9) (1998) 700–703.
[7] H.W. Hugosson, U. Jansson, B. Johansson, O. Eriksson, Phase stability diagrams of transition metal carbides, a theoretical study, Chem. Phys. Lett. 333 (6) (2001) 444–450.
[8] K. Bobzin, Benetzungs- und Korrosionsverhalten von PVD-beschichteten Werkstoffen für den Einsatz in umweltverträglichen Tribosystemen, Dissertation, RWTH Aachen, 2000.

[9] F. Klocke, H.W. Raedt, Formulation and testing of optimised coating properties with regard to tribological performance in cold forging and fine blanking applications, Int. J. Refract. Met. Hard Mater. 19 (2001) 495–505.
[10] DIN EN 10002-1, Metallic materials – tensile testing. Part 1. Method of test at ambient temperature, December 2001.
[11] E. Lugscheider, K. Bobzin, M. Maes, H. Murrenhoff, D. van Bebber, W. Dott, A. Eisenträger, K. Michel, Transferring tribological functions of lubricants to the surface of components by means of PVD technology, “THE” Coatings, Thessaloniki, Greece, 28./29.11.2002.
[12] E. Lugscheider, K. Bobzin, Wettability of PVD compound materials by lubricants, Surf. Coat. 165 (2003) 51–57.